applied sciences

MDPI

Article

Preliminary Study of New Sustainable, Alkali-Activated Cements Using the Residual Fraction of the Glass Cullet Recycling as Precursor

Jessica Giro-Paloma, Alex Maldonado-Alameda, Anna Alfocea-Roig, Jofre Mañosa, Josep Maria Chimenos and Joan Formosa *

Departament de Ciència de Materials i Química Física, Universitat de Barcelona, C/Martí i Franquès, 1, 08028 Barcelona, Spain; jessicagiro@ub.edu (J.G.-P.); alex.maldonado@ub.edu (A.M.-A.); annaalfocea@ub.edu (A.A.-R.); jofremanosa@ub.edu (J.M.); chimenos@ub.edu (J.M.C.)
* Correspondence: joanformosa@ub.edu; Tel.: +34-93-402-1316

Featured Application: The use of a residue that is currently disposed of in landfills was considered in this study, to obtain binder materials more sustainable and respectful to the environment. The recycling glass industry is identified as a model to advance towards a circular economy. The recycling glass rate in Europe is around 74%; meanwhile, in Spain it is approximately 70%, as reported elsewhere. However, in Spain, there is a problem with a residue obtained during the glass recycling process. The residue is named CSP (ceramic, stone, and porcelain). The results of this contribution show that is possible to use this residue as the precursor for developing alkali-activated cements (AAC). Due to the small amount of aluminum in CSP, it is desirable to use it as a non-hydraulic binder for specific purposes, such as prefabrication, decoration, insulation walls, or flooring material. Otherwise, for future works, it will be necessary to include aluminum for hydraulic binder development.

Abstract: During the glass selection process by optical sorting equipment, a rejection material called CSP (ceramic, stone, and porcelain) is generated, which is lower than 2 wt % of the glass cullet collected in Catalonia (Spain). Although this process should only separate non-glass impurities from the glass cullet, around 84 wt % of glass is found in the CSP. The CSP characterization reveals that CSP is mainly compound by SiO_2, Al_2O_3, alkali metals, and CaO, which are key components for the alkali-activated cement (AAC) development. Consequently, this study is focused on the potential of CSP as a precursor to synthesize AAC. The concentration of the alkali activator (NaOH: 1 M, 4 M, and 8 M) and the liquid-to-solid (L/S) ratio were tested in the formulation of the AAC. The AAC specimens at 28 days cured were evaluated using X-ray diffraction (XRD), Fourier transform infrared spectroscopy (FIR), scanning electron microscopy (SEM), apparent density (ρ_{app}), and compressive strength (σ_s). The results obtained showed that the L/S of 0.5 and 4.0 M for NaOH concentration are the best conditions, due to the mechanical properties (ρ_{app} = 1.75 g·cm^{-3}; σ_s = 52.8 MPa), cohesion (SEM), and formed phases (XRD and FT-IR). Therefore, CSP can be a precursor for developing new, sustainable binders.

Keywords: sustainable binder; alkali-activated cement; residue; CSP; municipal waste management

Citation: Giro-Paloma, J.; Maldonado-Alameda, A.; Alfocea-Roig, A.; Mañosa, J.; Chimenos, J.M.; Formosa, J. Preliminary Study of New Sustainable, Alkali-Activated Cements Using the Residual Fraction of the Glass Cullet Recycling as Precursor. *Appl. Sci.* **2021**, *11*, 3528. https://doi.org/10.3390/app11083528

Academic Editor: Joamin Gonzalez-Gutierrez

Received: 17 March 2021
Accepted: 13 April 2021
Published: 15 April 2021

1. Introduction

An important challenge in the present society is proper management of waste, which is generated both in urban and industrial areas. The new environmental European Union (EU) policies in the waste management field [1], based on the concept of the circular economy, are focused on recycling and recovery promotion. On the other hand, the EU is making efforts to reduce CO_2 emissions and energy consumption, which are growing exponentially. One of the solutions to overcome the above-mentioned problems is the

development of new materials more respectful to the environment, as well as secondary raw material usage in its manufacture.

In the past few decades, regarding the framework of building material applications, there has been a commitment to reduce greenhouse gas (GHG) emissions by using materials that have a low carbon emission associated with their manufacture. In this sense, one of the most polluting materials during its manufacturing process is ordinary Portland cement (OPC). The OPC industry is responsible for 7% of global CO_2 emissions and 3% of global energy consumption. In this regard, the cement industry must face the challenge of producing materials more sustainably to reduce the levels of contamination and environmental degradation. Nowadays, different alternative cements are being studied to reduce CO_2 emissions and energy consumption during the manufacturing process [2–6], as well as being able to incorporate waste into their formulations by contributing to the EU's strategic policies by the year 2050.

By the year 2030, the recycling packaging rate is expected to reach at least 75% [7]. Up to now, Belgium, Denmark, and the Czech Republic have accomplished this target, although there are also some countries close to achieving it (e.g., Spain) [8]. If attention is focused on the recycling glass rate, in Europe around 74% is accomplished [9], and above 70% in Spain [8]. The energy and natural resource savings, low emission of GHGs, water pollution reduction, and high recyclability of glass (as well as its capacity to be recycled infinite times without losing its properties) [10], turn the recycling glass industry into an example of sustainability and circular economy. Unfortunately, it exists in an improper fraction, composed of glass and non-glass materials, which are found in the glass treatment process and hinder its recycling. In Catalonia, the improper fraction is estimated to be around 2 wt % of the total glass cullet collected in the separate curbside containers [11]. The most common improper are polyethylene terephthalate (PET) containers, ceramics, porcelain (cups and plates), and metal waste associated with tin and bottle caps. Elimination is relatively simple for metallic and plastic remains by using electromagnets and mechanical separators [12], respectively. However, in the case of ceramics and porcelain, their separation becomes a difficult task. In addition, the elimination of ceramics and porcelain is crucial for the subsequent recycling process, since its presence increases the glass melting temperature and can cause defects in the new container glass [13]. There is a European standard focused on minimizing these problems, which only considers the content of 20 g of ceramic or porcelain per ton of glass to be recycled [14], and it is not inconceivable that this would fall to 15 $g \cdot t^{-1}$. For the separation of these materials, the use of special optical sorting equipment is necessary, by using the laser, X-ray techniques, or optical cameras, allows the removal of non-glass contaminants, as well as sorting of mixed glass by color, obtaining a waste fraction known as CSP (ceramic, stone, and porcelain) [15]. Nevertheless, CSP contains a high amount of glass because the sorting equipment does not recognize as translucent elements glass fragments with labels or necks, or bottle bottoms. The CSP residue contains approximately 80 wt % of glass, around 4 wt % of ceramic, and 4 wt % of porcelain; the remaining components are small pieces of metals, polymers, papers, and organic materials. According to the Catalan recycling glass companies, around 4–5 wt % of the recycled glass is CSP, which is more than 30,000 t of CSP per year in Catalonia. Currently, as this residue cannot be valorized, the main destination of CSP in Spain is landfill, where accessibility in the EU is increasingly restricted [16] due to the environmental problems [17–20] generated by the waste deposits. In recent years, to increase sustainable and environmental criteria, the authors seek possible potential uses of this particular residue [21]. Regarding the elemental composition of CSP, it is rich in silicon, alkali metals, and to a lesser extent aluminosilicate (e.g., mullite), making it a suitable raw material to obtain alkali-activated cements (AAC) [22,23]. Obtaining AAC consists of the reaction of an aluminosilicate powder precursor with a highly alkaline activator solution to form sodium aluminosilicate hydrate (NASH; when CaO amount on precursor < 10%) or calcium aluminosilicate hydrate (CASH; when CaO amount on precursor > 10%) gels [23]. Also, it is possible to obtain CSH (calcium silicate hydrate) gel depending on the amount of the precursors [24]. The result of

these reactions, after a proper curing time and temperature, is a compact solid with good mechanical properties. AAC are considered as a sustainable alternative to OPC, due to low carbon emissions during their manufacture, as well as their appropriate mechanical properties, chemical stability, acid resistance, and fire resistance [19], among others. There are several publications about the compressive strength of AAC developed by using glass wastes as precursors, such as that by Zhu et al., where 70 MPa were reported when the specimens were cured at 75 °C and 98% relative humidity for 3 days [25]. Tho-In et al. obtained compressive strength values around 49 Mpa after combining glass wastes with fly ash (FA); the samples were cured at 60 °C in an oven for 48 h, and consequently cured at 23–25 °C and 50% relative humidity to be tested at 7 days [26]. Xiao et al. obtained around 30 MPa at 28 days when FA and glass waste were combined in a 1:3 weight ratio with 5 M NaOH solution and cured at room temperature [27].

A large variety of industrial waste and by-products can be used as precursors, with the purpose of developing new sustainable binders or AAC [28,29]. All these alkali-activated waste solid precursors are rich in silica and alumina, with the highest possible amorphization degree. Hence, there are several publications, including urban and industrial waste glass, which is specifically glass as a precursor in alkaline activation [30–32].

However, unlike what happens with this kind of waste glass, CSP is a residue that is discarded in the glass cullet recycling industry, and for this reason, it is currently disposed of in landfills because of its 20 g of ceramic or porcelain per ton of glass content. In this regard, the use of CSP as a raw material in the AAC formulations must allow valorizing this rejected fraction generated during the glass recycling process. Aiming to contribute to the development of new sustainable materials, the present work was focused on studying CSP for its valorization and using it in high-benefit applications that definitively close the cycle of glass recycling. In this way, the main objective of the present study was to evaluate the potential of CSP for its use as a precursor in the synthesis of AAC (as sustainable cement), with NaOH as an activator. Consequently, different formulations from CSP generated in a glass treatment plant to develop sustainable binders were studied to reduce the material disposed of in landfills (with important environmental and economic advantages), and to obtain more ecological and respectful cements with the environment. The chemical composition and microstructure of the AAC formulations were characterized by Fourier transform infrared spectroscopy (FTIR) by using attenuated total reflectance sampling technique (ATR), X-ray diffraction (XRD), and scanning electron microscopy (SEM). The physical and mechanical characterization of the AAC formulations was evaluated by the apparent density (ρ_{app}), and compressive strength (σ_c) at 28 days of curing. These were determined at the age of 28 days for a better understanding of mechanical properties. For this purpose, using CSP as a precursor, different concentrations of the alkaline activator solutions were considered, as well as different precursor–activator ratios.

2. Materials and Methods

The CSP sample was collected from the glass treatment plant Daniel Rosas, S.A., located in Barcelona (Spain). This plant manages 90,000 t per year of glass cullet, collected in curbside containers. The particle size distribution (Figure 1a) and the percentage composition (Figure 1b) in mass were determined after cleaning the sample with soap, to eliminate the remains of dirt and ferments produced during the deposit of CSP in the treatment plant. As can be observed in Figure 1a, the highest percentage (wt %) for CSP was the 8–16 mm particle size fraction, followed by the size fraction > 16 mm. On the other hand, Figure 1b shows glass as the main component in CSP.

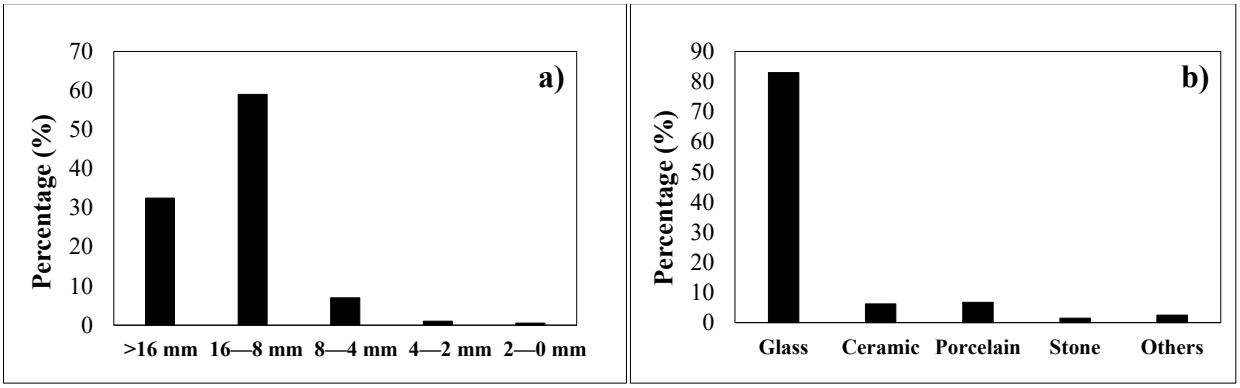

Figure 1. CSP (ceramic, stone, and porcelain) waste as raw material and as an alkali-activated cement (AAC) precursor: (**a**) Particle size distribution in mass percentage; (**b**) CSP composition (wt %).

Moreover, to improve the reactivity for AAC synthesis, the CSP sample was crushed and milled, using a ball mill, until CSP particle sizes were below 80 μm. The particle size distribution (PSD) of the CSP used as precursor raw material (i.e., after crushing and milling below 80 μm) was determined by using a Beckman Coulter LS^{TM} 13 320. Additionally, the CSP powder semi-quantitative elemental analysis was carried out by a Panalytical Philips PW 2400 sequential X-ray fluorescence (XRF) spectrophotometer equipped with the software UniQuant V5.0. In addition, X-ray diffraction (XRD) analysis was conducted to determine the crystalline phases of CSP and the different AAC formulations using a Bragg–Brentano Siemens D-500 powder diffractometer device with CuKα radiation. Fourier transform infrared spectroscopy (FTIR) by using the attenuated total reflectance sampling technique (ATR) was performed to compare the CSP initial powder structure before the AAC composition, employing Spectrum Two equipment from Perkin Elmer supported by a Dynascan interferometer and OpticsGuard technology. FTIR equipment is optimized by a wavelength range between 4000 cm^{-1} and 500 cm^{-1}, and its standard spectral resolution is 0.5 cm^{-1}.

Different alkaline solutions were studied as activators to elucidate the effect of the activator concentration in the AAC synthesis. For this purpose, various concentrations of sodium hydroxide solutions (1 M, 4 M, and 8 M) were prepared by using sodium hydroxide pearls (Labkem) dissolved in deionized water. Sodium hydroxide concentrations were chosen by following the conclusions reported by Cyr et al. when NaOH is used for geopolymer mortars made of glass cullet [33].

The AAC specimens using CSP as precursor were formulated by mixing the CSP powder (below 80 μm) with the NaOH solutions as an alkaline activator, according to the designed formulations shown in Table 1. The same amount of CSP (16 g) was used for each formulation, and different amounts of NaOH solutions (8.0 and 9.6 g) were added to the CSP powder to obtain the two liquid-to-solid (L/S) ratios under study: 0.5 and 0.6. L/S ratios were selected after preliminary tests for obtaining proper workability of the mixtures.

Table 1. The AAC mixture composition.

Reference	CSP (g)	NaOH Solution (g)			L/S (wt %)
		1 M	4 M	8 M	
05LS1M	16	8.0			0.5
05LS4M	16		8.0		0.5
05LS8M	16			8.0	0.5
06LS1M	16	9.6			0.6
06LS4M	16		9.6		0.6
06LS8M	16			9.6	0.6

The mixing process between CSP powder and the alkaline solution consisted of slowly adding the CSP powder to the NaOH solution while mixing mechanically for 5 min, thus contributing to its activation. Later, the mixed paste was cast into plastic molds and vibrated for 5 s to compact the mixture. The molds were sealed in a plastic bag to minimize the moisture loss for 3 days at 40 °C ± 1 °C (relative humidity of 10% ± 5%) in a climate chamber. Afterward, the specimens were unsealed, unmolded, and cured in the same work conditions up to the age to be tested (28 days). As reported by Cyr et al. [34], the proper curing temperature range to elaborate AAC with a glassy nature precursor was between 40 °C and 60 °C. Three cylindrical, prism-shaped specimens (27 mm diameter and 15 mm height) were prepared for each formulation, as shown in Figure 2. The specimens were used for compression strength after 28 days, as shown in the scheme in Figure 2. Afterward, the obtained fragments after the compression tests were used to determine the apparent density at the same age. Finally, the physico-chemical characterization of the AAC samples was carried out with the same obtained fragments.

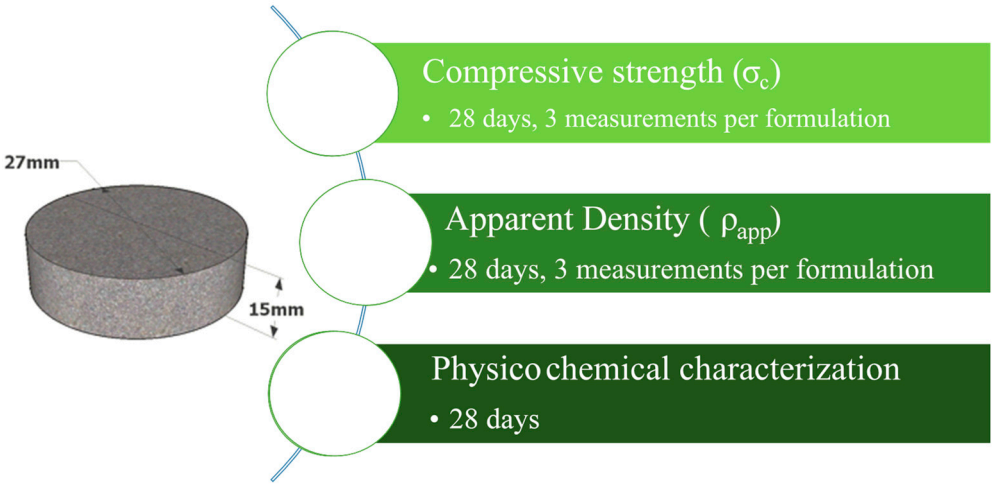

Figure 2. Experimental tests flowsheet.

The physical and mechanical characterization of AAC formulations was conducted by following several standards. The apparent density (ρ_{app}), according to the Spanish standard UNE 83-312-90, based on the Archimedes principle, was determined at the age of 28 days for a better understanding of mechanical properties. The compressive strength (σ_c) at 28 days of curing was determined for each formulation of AAC in a mechanical testing machine MUTC-200 from Incotecnic, at a loading rate of 240 kg·s^{-1}, by following the standard EN 196-1.

Additionally, scanning electron microscope (SEM) observation of AAC formulations coated in carbon was performed by using a Quanta 200 FEI, XTE 325/D8395, obtaining micrographs by backscattered and secondary electrons.

3. Results

3.1. CSP Characterization

CSP was previously crushed and milled to particle sizes below 80 µm to improve the reactivity for the AAC synthesis (see the previous section). A proper physico-chemical characterization of CSP allows us to determine the potential reaction with NaOH. The PSD is shown in Figure 3. As can be seen, CSP used as a precursor presents a bimodal distribution, reaching the maximum particle size at 30 µm and 10 µm. As was expected, all the particles were below 80 µm, because of the previous conditioning process.

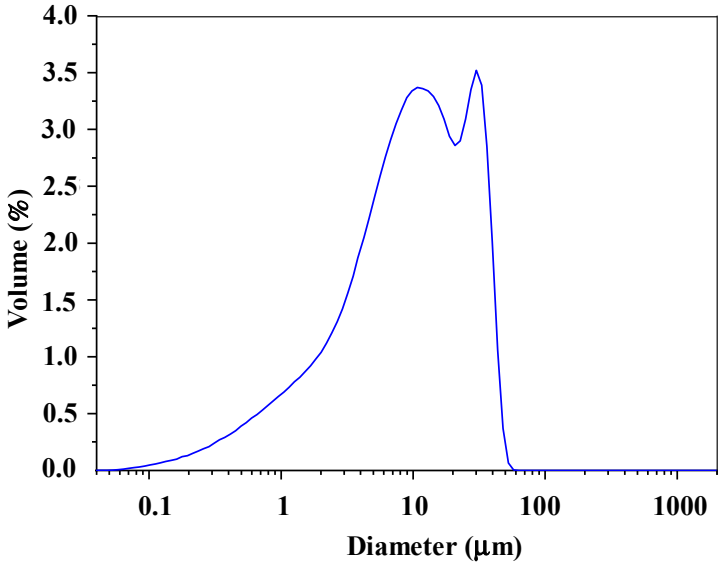

Figure 3. Particle size distribution of the CSP after milling used as raw material.

The main elemental oxide composition in CSP powder, determined by employing XRF, is shown in Table 2. As expected, considering the high glass content in CSP, the main oxides found were SiO_2, Na_2O, CaO, and Al_2O_3, which are the same components of soda-lime glass [33,35]. In addition, XRD and FTIR were evaluated for CSP raw material. However, the results are shown in the next section for better comprehension and interpretation of the obtained results when AACs were prepared with milled CSP and NaOH.

Table 2. X-ray fluorescence (XRF) results from the CSP raw material.

Compounds	CSP (wt %)
SiO_2	70.78
Na_2O	11.15
CaO	9.37
Al_2O_3	4.81
MgO	1.61
K_2O	0.94
Fe_2O_3	0.57
TiO_2	0.13
P_2O_5	0.04
MnO	0.02
LOI	0.99

3.2. AAC Characterization

3.2.1. AAC Physico-Chemical Characterization

The XRD patterns of CSP and AAC, formulated as a function of the NaOH concentration and L/S ratio, are shown in Figure 4. It should be noted that no significant differences were found between the XRD patterns of both S/L (0.5 and 0.6) ratios. All the diffractograms showed an important halo (between the 2θ range from 15° and 35°) corresponding to the amorphous phases (vitreous phases) of the CSP, as well as the presence of quartz (PDF-01-085-0457, most important peaks for the identification of this crystalline phase at 26.625° and 20.827°) and mullite (PDF-01-079-1457, most important peak for the identification of this crystalline phase at 16.441°) as the main crystalline phases. The sodium carbonate (PDF-01-072-0628, mainly because of the peaks at 37.985° and 30.149°) in small amounts were detected in 4 M formulations (05LS4M and 06LS4M), and in higher amounts were also detected for the 8 M formulations (05LS8M and 06LS8M). In addition, calcium silicate hydrate (PDF-01-074-1995) was detected for 4 M formulations and potentially

presented in 8M formulations. Considering the clearest presence of sodium carbonate in 8 M formulations and the evidence of calcium silicate hydrate in 4 M formulations, it can be assumed that the higher the NaOH concentration, the higher the amount of sodium carbonate, and the lower the presence of calcium silicate hydrate. The presence of calcium silicate hydrate is related to CSH gel, which is better determined in 4 M formulations by the peak at 31.650°, probably due to a lower presence of sodium carbonate. Notice that the higher the alkali concentration, the higher the displacement of amorphous halo, due to the formation of NASH gel [33].

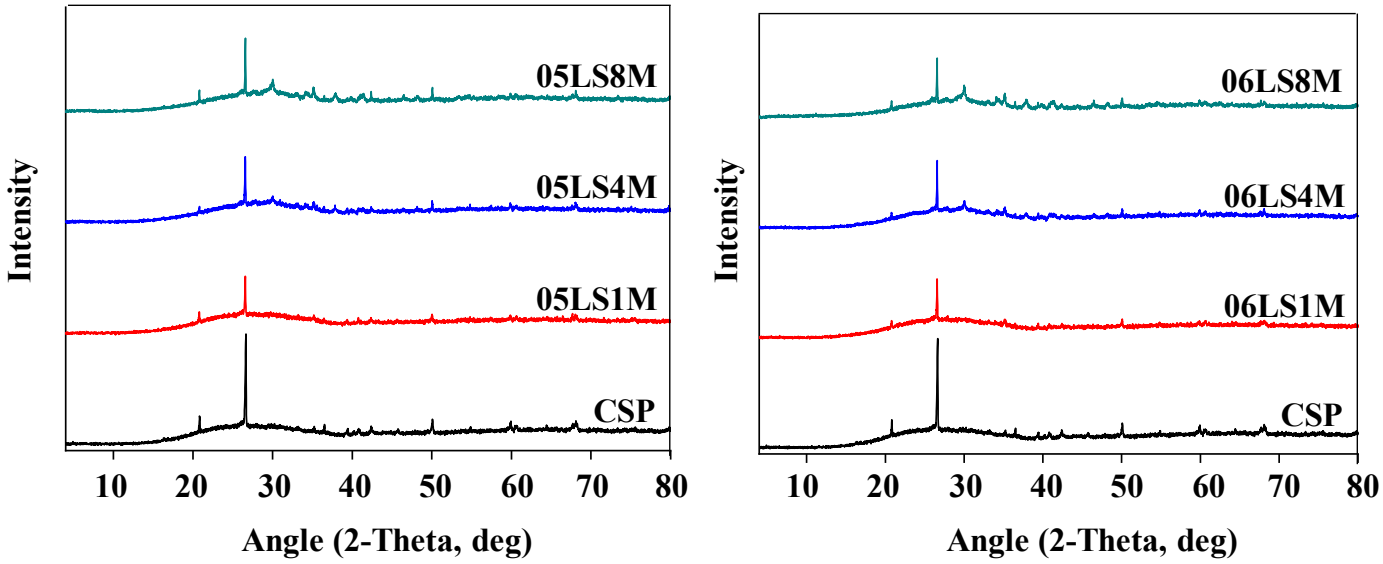

Figure 4. X-ray diffraction (XRD) results for the CSP precursor and the different AAC formulations obtained depending on the liquid-to-solid ratio (L/S) ratios (0.5 and 0.6) and the NaOH concentration.

Regarding FTIR characterization, Figure 5 shows the variation of some IR bands depending on the different NaOH formulations, as well as the different L/S ratios. Again, for the same NaOH concentration, it should be noted that no significant differences were found between the FTIR spectra of both L/S (0.5 and 0.6) ratios. A displacement to lower frequencies in the peak around 1000 cm^{-1} can be seen from CSP concerning the different AAC formulations, because of the formation of NASH gel [36,37]. These displacements indicate that the vitreous component was reacting with the NaOH, and therefore, new products of the reaction were formed [38]. As can be seen in the zoomed-in areas of Figure 6, the formulations of 4 M NaOH concentration present slightly lower frequencies than the 8 M NaOH concentration formulations. In addition, three main peaks in both spectra can be observed: (i) a peak at 1400 cm^{-1}, due to the stretching vibration of CO_3^{2-}, in 1 M, 4 M, and 8 M formulations; (ii) a peak between 1020 cm^{-1} and 970 cm^{-1}, because of the asymmetrical stretching peak of Si–O–Si and Si–O–Al in CSP raw material and AAC formulated with 1 M, 4 M, and 8 M NaOH; (iii) a peak at 885 cm^{-1}, which corresponds to the CO_3^{2-} bending vibration in AAC with 1 M, 4 M, and 8 M NaOH.

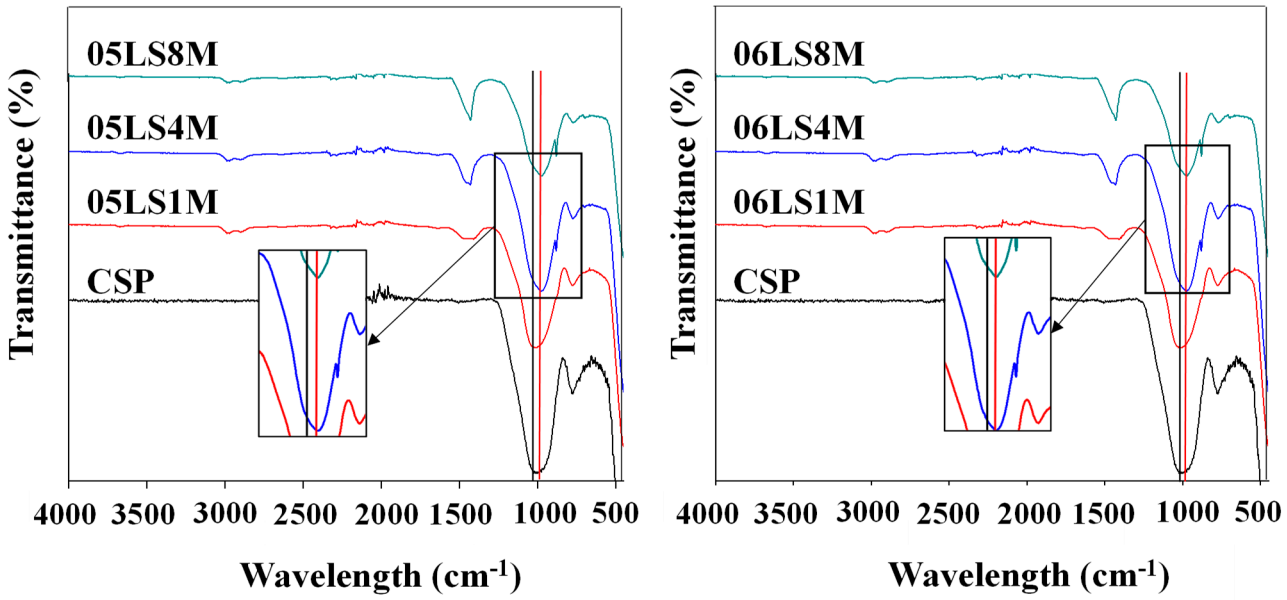

Figure 5. FTIR spectra results for the CSP precursor and the different AAC formulations obtained, depending on the L/S ratios (0.5 and 0.6) and the NaOH concentration.

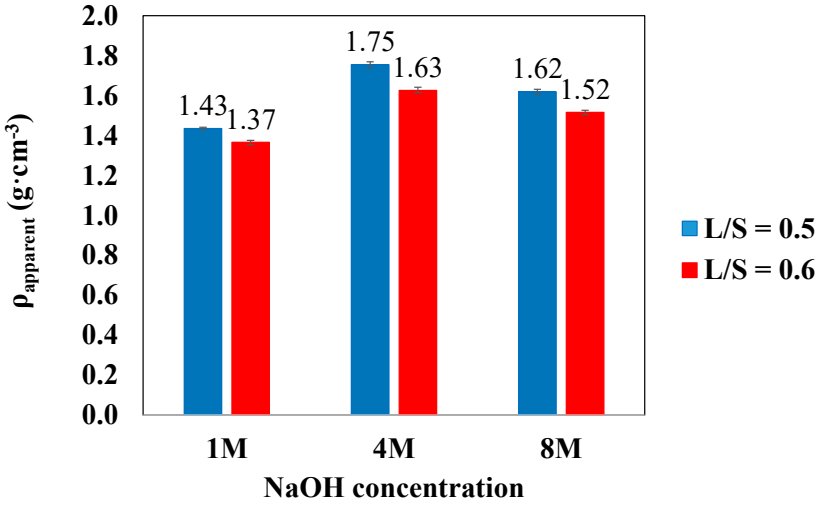

Figure 6. Apparent density results of the different AAC formulations obtained, depending on the L/S ratios (0.5 and 0.6) and the NaOH concentration.

3.2.2. AAC Physical and Mechanical Characterization

An in-depth physical and mechanical characterization was conducted. To perform a mechanical study of the different formulations depending on the L/S ratios, the apparent density (ρ_{app}) and the compressive strength (σ_s) were also evaluated. When analyzing the results performed by triplicate of the ρ_{app} exhibited in Figure 6, as expected, an increase of the L/S ratio (from 0.5 to 0.6) led to a decrease of the ρ_{app}, due to the greater amount of water in the AAC formulations. Moreover, when comparing the results as a function of NaOH concentration (1 M, 4 M, and 8 M), it can be noticed that samples with the 4 M concentration have higher values, while samples with the 1 M concentration have lower values. On one hand, the 05LS4M formulation was the densest (more compact), and on the other hand, the 05LS1M was the least dense. Hence, regarding the density results, the 05LS4M formulation would be expected that presents better behavior from a mechanical point of view.

In this way, it was considered relevant to evaluate the mechanical properties concerning the compressive strength (σ_s), as constructive purposes were the main use for the AAC

formulations. The results shown in Figure 7 demonstrate a decrease in the compressive strength when increasing the L/S ratio from 0.5 to 0.6, due to the greater amount of water needed in the formulations. Regarding the results as a function of NaOH concentration, it the highest values were observed in 4 M samples, and the lowest values in 1 M samples. Then the most compact and cohesive formulation had the highest compression strength values, and the most disaggregated formulation (see Figure 6) had the lowest compression strength results. Accordingly, the 05LS4M formulation presented again better results from a mechanical point of view. In other words, the apparent density and compressive strength results are in agreement. The compressive strength obtained in this research is remarkable when compared to other studies. As mentioned, Zhu et al. obtained 70 MPa [25], but the samples were cured at 75 °C. Tho-In et al. obtained around 49 MPa [26], but the glass waste was combined with fly ash (FA), which apports aluminum to the gel, and the samples were cured at 60 °C. Xiao et al. obtained around 30 MPa at 28 days [27]; in this case, the samples were cured at room temperature, but once again they used FA.

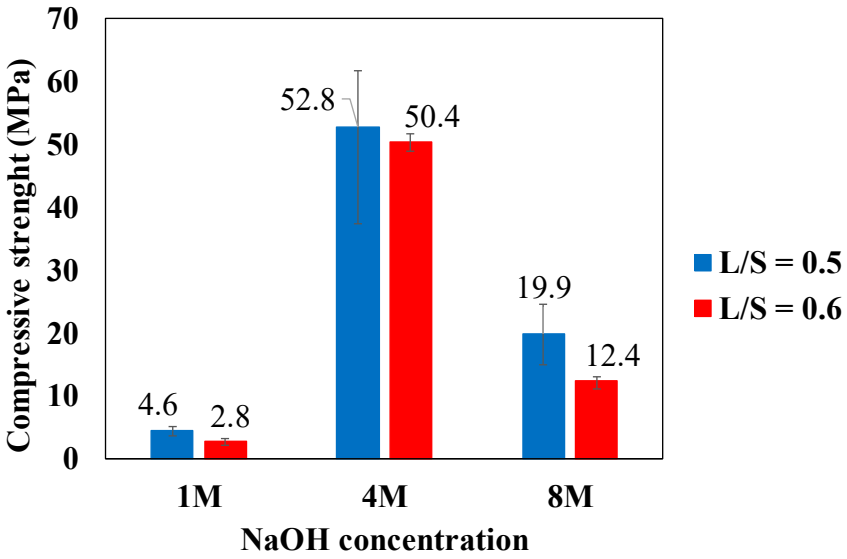

Figure 7. Compressive strength (σ_s) results of the different AAC formulations obtained depending on the L/S ratios (0.5 and 0.6) and the NaOH concentration.

These results are related to the abovementioned results of XRD and FTIR. On the one hand, XRD revealed the presence of CSH in 4 M formulations, and better evidence of sodium carbonate in 8 M formulations. As it is reported [24], when the activator concentration is high, it is difficult to produce the precipitation of hydrated calcium silicate. The presence of CSH in 4 M formulations improves mechanical properties. On the other hand, FTIR reveals slightly lower frequencies (peak between 1020 cm^{-1} and 970 cm^{-1}) for 4 M, which is related to NASH formation; this could be attributed to a better formation of NASH gel for 4 M formulations. In this manner, considering physical, mechanical, and microstructural results, it could be assumed that 4 M formulations must present more CSH and NASH phases than 1 M and 8 M formulations.

The main aim for the SEM study in the present manuscript is focused on the evaluation of AAC cohesion. The AAC formulations for L/S = 0.5 were selected to be observed by SEM using secondary electrons, as is shown in Figure 8. Formulations with L/S = 0.5 were selected for the SEM evaluation due to the higher σ_s and ρ_{app} values compared with L/S = 0.6 formulations. The specimens were cut to study the cohesion of several inner zones of the different formulations (05LS1M, 05LS4M, 05LS8M). Figure 8 shows representative micrographs of the inner zones of each formulation. It can be observed that the specimen formulated using 4 M NaOH was the one that presented proper cohesion, while those formulated using 1 M and 8 M NaOH showed less cohesion with disaggregated particles (more pronounced in 1 M NaOH formulation), as can be denoted in Figure 8. The cohesion

and the homogeneous structure of the binder matrix allowed a better understanding of the mechanical properties of the AAC specimens and the values determined by the apparent density.

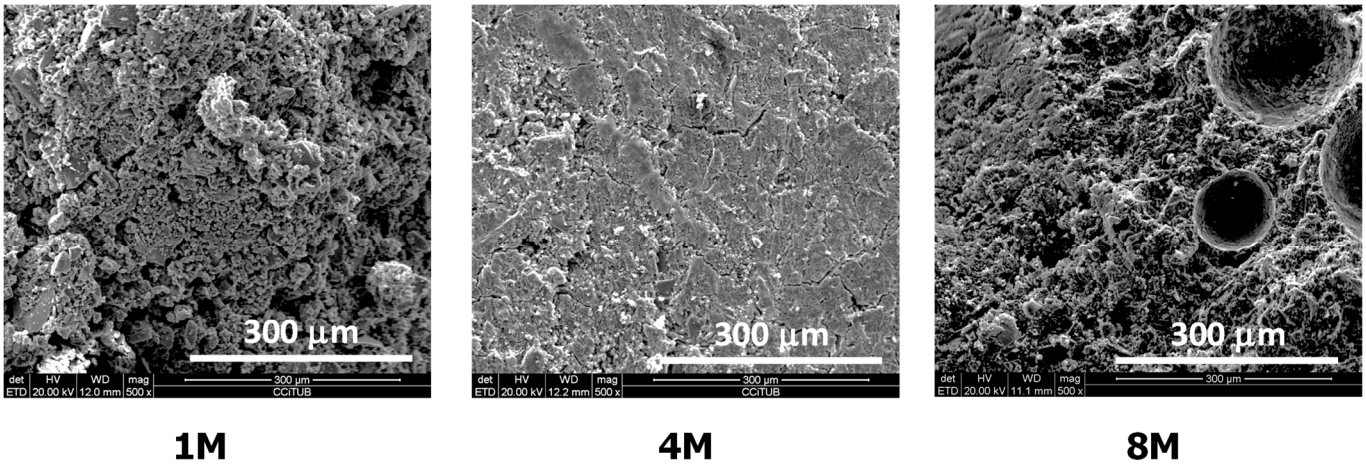

Figure 8. SEM micrographs of the AAC formulations with an L/S ratio of 0.5 (i.e., 1 M = 05LS1M, 4 M = 05LS4M, 8 M = 05LS8M).

4. Conclusions

To develop new, sustainable materials and to reuse the CSP fraction generated during glass cullet recycling, different AAC formulations have been developed. These newly formulated sustainable binders contained the CSP as a sole precursor, while the different concentrations of NaOH was used as activator solutions. Glass is the main component of the CSP fraction, with a high level of amorphization degree and SiO_2, Na_2O, CaO, and Al_2O_3 as the main components; these are all key components for alkali-activated cement (AAC) development. The XRD pattern of the AAC, formulated using CSP as a sole precursor, showed a displacement of the amorphous halo when increasing the alkali concentration of the activator, due to the potential formation of NASH gel. Likewise, the FTIR results also indicated a displacement in the peak around 1000 cm^{-1} (Si–O–Si) from CSP concerning the different AAC formulations, regarding again the formation of N-A-S-H gel. After the SEM observation, it was concluded that the AAC formulated with the NaOH 4 M and L/S = 0.5 were the specimens with proper cohesion and integrity of the matrix binder. This result was in accordance with the apparent density and compressive strength. On the one hand, a decrease was observed in the apparent density when increasing the L/S ratio from 0.5 to 0.6, and higher values were obtained in the 4 M NaOH formulations. On the other hand, a decrease in the compressive strength was tested when increasing the L/S ratio from 0.5 to 0.6, and an important increase was achieved in the 4 M NaOH formulations. Accordingly, it was demonstrated that CSP can be employed as a precursor for alkaline cement formulation for constructive purposes, considering as key parameters the activator concentration and L/S ratios, as these affect the physical and mechanical properties of the AAC obtained.

This research sheds light on the potential use of the CSP as a precursor for AAC. It should be emphasized that CSP is a residue in Spain and is disposed of in landfills because it is not useful for the recycling glass cullet industry. Therefore, the present research is a relevant solution for enhancing sustainable and environmental criteria, as well as following a circular economy strategy.

Author Contributions: Conceptualization, A.M.-A., J.G.-P. and J.F.; methodology, A.M.-A., J.G.-P., J.M.C. and J.F.; software, A.A.-R., J.M., J.G.-P. and J.F.; formal analysis, A.M.-A., J.G.-P. and J.F.; investigation, A.M.-A., J.G.-P., A.A.-R. and J.M.; writing—original draft preparation, J.G.-P. and J.F.; writing—review and editing, A.M.-A. and J.M.C.; supervision, J.G.-P. and J.F.; funding acquisition, J.M.C. and J.F. All authors have read and agreed to the published version of the manuscript.

Funding: This research was partially funded by the Spanish Government (BIA2017-83912-C2-1-R). Mr. Alex Maldonado-Alameda and Mr. Jofre Mañosa are grateful to the Catalan Government for their research Grants, FI-DGR 2017 and FI 2020, respectively.

Institutional Review Board Statement: Not applicable.

Informed Consent Statement: Not applicable.

Acknowledgments: The authors would like to thank the Catalan Government for the quality accreditation given to their research group DIOPMA (2017 SGR 118). The authors also want to thank Daniel Rosas S.A. company for supplying the CSP sample. Jessica Giro-Paloma is a Serra Húnter Fellow.

Conflicts of Interest: The authors declare no conflict of interest.

References

1. European Commission. An EU Action Plan for the Circular Economy. 2015. Available online: https://ec.europa.eu/environment/strategy/circular-economy-action-plan_en (accessed on 14 April 2021).
2. Giro-Paloma, J.; Maldonado-Alameda, A.; Formosa, J.; Barbieri, L.; Chimenos, J.M.; Lancellotti, I. Geopolymers based on the valorization of Municipal Solid Waste Incineration residues. *IOP Conf. Ser. Mater. Sci. Eng.* **2017**, *251*, 012125. [CrossRef]
3. Maldonado-Alameda, A.; Lacasta, A.M.; Giro-Paloma, J.; Chimenos, J.M.; Haurie, L.; Formosa, J. Magnesium phosphate cements formulated with low grade magnesium oxide incorporating phase change materials for thermal energy storage. *Constr. Build. Mater.* **2017**, *155*. [CrossRef]
4. McLellan, B.C.; Williams, R.P.; Lay, J.; Van Riessen, A.; Corder, G.D. Costs and carbon emissions for geopolymer pastes in comparison to ordinary portland cement. *J. Clean. Prod.* **2011**, *19*, 1080–1090. [CrossRef]
5. Lancellotti, I.; Cannio, M.; Bollino, F.; Catauro, M.; Barbieri, L.; Leonelli, C. Geopolymers: An option for the valorization of incinerator bottom ash derived "end of waste". *Ceram. Int.* **2015**, *41*, 2116–2123. [CrossRef]
6. Morales, M.; Formosa, J.; Xuriguera, E.; Niubó, M.; Segarra, M.; Chimenos, J.M. Elastic modulus of a chemically bonded phosphate ceramic formulated with low-grade magnesium oxide determined by Nanoindentation. *Ceram. Int.* **2015**, *41*. [CrossRef]
7. European Commission. Directive of the European Parliament and of the Council—Amending Directive 94/62/EC on Packaging and Packaging Waste. 2015. Available online: https://www.eea.europa.eu/policy-documents/directive-eu-2018-852-of (accessed on 14 April 2021).
8. Eurostat, Recycling Rates for Glass Packaging Waste. 2018. Available online: https://ec.europa.eu/eurostat/databrowser/product/view/ENV_WASPACR (accessed on 2 February 2018).
9. The European Container Glass Federation: Glass Packaging Closed Loop Recycling Up to 74% in the EU. 2016. Available online: https://feve.org/glass-packaging-closed-loop-recycling-74-eu/ (accessed on 14 April 2021).
10. Beerkens, R.; Kers, G.; Van Santen, E.; TNO Glass Group. Recycling of Post-Consumer Glass: Energy Savings, CO2 Emissions Reduction, Effects on Glass Quality and Glass Melting. Available online: https://repository.tno.nl/islandora/object/uuid%3Ae2aab36a-2fa0-4cff-b085-f34d992aed79 (accessed on 14 April 2021).
11. Agència de Residus de Catalunya. *Balanç de les Dades Estadístiques de Residus Municipals de L'any 2016*; Agència de Residus de Catalunya: Barcelona, Spain, 2017.
12. Marını, P.; Bellopede, R.; Zanottı, G.; Ramon, V. Waste of the secondary glass waste (glass waste 3): New solutions for a sustainable industrial recovery. In Proceedings of the 15th International Conference on Environmental Science and Technology, Rhodes, Greece, 31 August–2 September 2017.
13. Beerkens, R.; Van Santen, E. Recycling in container glass production present problems in European glass industry. In Proceedings of the 66th Conference on Glass Problems: Collection of Papers Presented at the 66th Conference on Glass Problems, The University of Illinois at Urbana-Champaign, Champaign, IL, USA, 24–26 October 2005; John Wiley & Sons: Hoboken, NJ, USA, 2004; pp. 181–202.
14. Dutch Waste Management Association. *Closing the Glass Recycling Loop*; Dutch Waste Management Association: Hertogenbosch, The Netherlands, 2015; pp. 1–5.
15. Mogensen GmbH &, Co. KG Glass Recycling. 2008. Available online: https://koasltd.com/ckfinder/userfiles/images/PDF/Glass_Recycling_2008.pdf (accessed on 14 April 2021).
16. European Commission. Directive of the European Parliament and of the Council—Amending Directive 2008/98/EC on Waste. 2015. Available online: https://eur-lex.europa.eu/legal-content/EN/TXT/?uri=CELEX%3A52015PC0595 (accessed on 14 April 2021).
17. Lou, X.F.; Nair, J. The impact of landfilling and composting on greenhouse gas emissions—A review. *Bioresour. Technol.* **2009**, *100*, 3792–3798. [CrossRef] [PubMed]

18. Kasassi, A.; Rakimbei, P.; Karagiannidis, A.; Zabaniotou, A.; Tsiouvaras, K.; Nastis, A.; Tzafeiropoulou, K. Soil contamination by heavy metals: Measurements from a closed unlined landfill. *Bioresour. Technol.* **2008**, *99*, 8578–8584. [CrossRef] [PubMed]
19. Assmuth, T.W.; Strandberg, T. Ground water contamination at Finnish landfills. *Water. Air. Soil Pollut.* **1993**, *69*, 179–199. [CrossRef]
20. Marijan, A.; Mikac, N.; Cosovic, B.; Prohic, E.; Soukup, V. The impact of contamination from a municipal solid waste landfill (Zagreb, Croatia) on underlying soil. *Water Sci. Technol.* **1998**, *37*, 203–210.
21. Huete-Hernández, S.; Maldonado-Alameda, A.; Giro-Paloma, J.; Chimenos, J.M.; Formosa, J. Fabrication of sustainable magnesium phosphate cement micromortar using design of experiments statistical modelling: Valorization of ceramic-stone-porcelain containing waste as filler. *Ceram. Int.* **2020**. [CrossRef]
22. Komnitsas, K.; Zaharaki, D. Geopolymerisation: A review and prospects for the minerals industry. *Miner. Eng.* **2007**, *20*, 1261–1277. [CrossRef]
23. Duxson, P.; Fernández-Jiménez, A.; Provis, J.L.; Lukey, G.C.; Palomo, A.; Van Deventer, J.S.J. Geopolymer technology: The current state of the art. *J. Mater. Sci.* **2007**, *42*, 2917–2933. [CrossRef]
24. Alonso, S.; Palomo, A. Calorimetric study of alkaline activation of calcium hydroxide-metakaolin solid mixtures. *Cem. Concr. Res.* **2001**, *31*, 25–30. [CrossRef]
25. Zhu, W.; Chen, X.; Zhao, A.; Struble, L.J.; Yang, E.H. Synthesis of high strength binders from alkali activation of glass materials from municipal solid waste incineration bottom ash. *J. Clean. Prod.* **2019**, *212*, 261–269. [CrossRef]
26. Tho-In, T.; Sata, V.; Boonserm, K.; Chindaprasirt, P. Compressive strength and microstructure analysis of geopolymer paste using waste glass powder and fly ash. *J. Clean. Prod.* **2016**, *172*, 2892–2898. [CrossRef]
27. Xiao, R.; Ma, Y.; Jiang, X.; Zhang, M.; Zhang, Y.; Wang, Y.; Huang, B.; He, Q. Strength, microstructure, efflorescence behavior and environmental impacts of waste glass geopolymers cured at ambient temperature. *J. Clean. Prod.* **2020**, *252*, 119610. [CrossRef]
28. Part, W.K.; Ramli, M.; Cheah, C.B. An overview on the influence of various factors on the properties of geopolymer concrete derived from industrial byproducts. *Handb. Low Carbon Concr.* **2016**, *77*, 263–334. [CrossRef]
29. Bernal, S.A.; Rodríguez, E.D.; Kirchheim, A.P.; Provis, J.L. Management and valorisation of wastes through use in producing alkali-activated cement materials. *J. Chem. Technol. Biotechnol.* **2016**, *91*, 2365–2388. [CrossRef]
30. Torres-Carrasco, M.; Puertas, F. Waste glass in the geopolymer preparation. Mechanical and microstructural characterisation. *J. Clean. Prod.* **2015**, *90*, 397–408. [CrossRef]
31. Torres-Carrasco, M.; Puertas, F. Waste glass as a precursor in alkaline activation: Chemical process and hydration products. *Constr. Build. Mater.* **2017**, *139*, 342–354. [CrossRef]
32. Lu, J.X.; Poon, C.S. Use of waste glass in alkali activated cement mortar. *Constr. Build. Mater.* **2018**, *160*, 399–407. [CrossRef]
33. Cyr, M.; Idir, R.; Poinot, T. Properties of inorganic polymer (geopolymer) mortars made of glass cullet. *J. Mater. Sci.* **2012**, *47*, 2782–2797. [CrossRef]
34. Cheng, J.; Xiao, Z.; Yang, K.; Wu, H. Viscosity, fragility and structure of Na_2O-CaO-Al_2O_3-SiO_2 glasses of increasing Al/Si ratio. *Ceram. Int.* **2013**, *39*, 4055–4062. [CrossRef]
35. Norton, M.G.; Carter, C.B. *Ceramic Materials Science and Engineering*; Springer: New York, NY, USA, 2007.
36. García-Lodeiro, I.; Fernández-Jiménez, A.; Palomo, A.; Macphe, D.E. Effect of calcium additions on N–A–S–H cementitious gels. *J. Am. Ceram. Soc.* **2010**, 1934–1940. [CrossRef]
37. Onisei, S.; Pontikes, Y.; Van Gerven, T.; Angelopoulos, G.N.; Velea, T.; Predica, V.; Moldovan, P. Synthesis of inorganic polymers using fly ash and primary lead slag. *J. Hazard. Mater.* **2012**, *205–206*, 101–110. [CrossRef] [PubMed]
38. Criado, M.; Aperador, W.; Sobrados, I. Microstructural and mechanical properties of alkali activated Colombian raw materials. *Materials* **2016**, *9*, 158. [CrossRef]